

Glia delimit shape changes of sensory neuron receptive endings in *C. elegans*

Carl Procko, Yun Lu and Shai Shaham*

SUMMARY

Neuronal receptive endings, such as dendritic spines and sensory protrusions, are structurally remodeled by experience. How receptive endings acquire their remodeled shapes is not well understood. In response to environmental stressors, the nematode *Caenorhabditis elegans* enters a diapause state, termed dauer, which is accompanied by remodeling of sensory neuron receptive endings. Here, we demonstrate that sensory receptive endings of the AWC neurons in dauers remodel in the confines of a compartment defined by the amphid sheath (AMsh) glial cell that envelops these endings. AMsh glia remodel concomitantly with and independently of AWC receptive endings to delimit AWC receptive ending growth. Remodeling of AMsh glia requires the OTD/OTX transcription factor TTX-1, the fusogen AFF-1 and probably the vascular endothelial growth factor (VEGFR)-related protein VER-1, all acting within the glial cell. *ver-1* expression requires direct binding of TTX-1 to *ver-1* regulatory sequences, and is induced in dauers and at high temperatures. Our results demonstrate that stimulus-induced changes in glial compartment size provide spatial constraints on neuronal receptive ending growth.

KEY WORDS: *C. elegans*, Glia, Sensory receptive ending

INTRODUCTION

Dendritic spines and sensory neuron protrusions are examples of specialized neuronal receptive endings that respond to extracellular cues. Spines detect and propagate signals evoked by presynaptic release of neurotransmitters, and sensory receptive endings process and interpret external sensory stimuli. Both structures exhibit striking similarities in function, shape and molecular constituents (Shaham, 2010), and both structures exhibit morphological plasticity. For example, during synaptogenesis in the mouse cerebellum, dendritic spines of Purkinje cells exhibit dynamic shape changes, with spines rapidly emerging, growing and retracting. The frequency of these shape changes decreases as development proceeds to establish a stable synaptic repertoire (Dunaevsky et al., 1999). Similarly, in the nematode *C. elegans*, the ciliated receptive endings of the AWB sensory neurons take on different morphologies in response to sensory deprivation (Mukhopadhyay et al., 2008), and perturbation of sensory signaling alters the shapes of receptive endings of AWC sensory neurons (Roayaie et al., 1998). Receptive ending shapes are also regulated by systemic cues. For example, dendritic spine number and density of rat hippocampal neurons is correlated with circulating estrogen levels (Woolley et al., 1990). Likewise, pheromonal cues trigger changes in the shapes of sensory neuron receptive endings in *C. elegans* (Albert and Riddle, 1983).

In response to environmental stressors, including high population density, low food abundance and high temperature, *C. elegans* enters a protective developmental stage, termed dauer, which is highly resistant to environmental insults. Dauer development is triggered by dauer pheromone, which promotes

systemic changes in physiology through insulin and TGF- β neuroendocrine signaling pathways (Kimura et al., 1997; Ren et al., 1996). Various cellular changes coincide with dauer entry, including remodeling of sensory receptive endings of the major sensory organs, the amphids (Albert and Riddle, 1983). The two amphids consist of bilateral pairs of neurons, each extending a dendrite that terminates in a ciliated sensory receptive ending at the nose-tip (Fig. 1A). In dauers, the spatially separated receptive endings of the AWC amphid neurons expand and overlap extensively (Albert and Riddle, 1983).

Dauer-induced AWC neuron remodeling offers unique advantages for studying receptive ending plasticity: it is inducible, reproducible, and can be studied in an organism with facile genetics and molecular biology.

Ensheathing the sensory ending of each AWC neuron is an amphid sheath (AMsh) glial cell. AMsh glia are also remodeled in dauers, such that the left and right AMsh glia expand and fuse at the nose-tip (Fig. 1B,C) (Albert and Riddle, 1983). Glia are the most abundant cell type in the human brain, and glia contribute extensively to nervous system disease (Canoll and Goldman, 2008; Ozawa et al., 1994; Shaham, 2005). However, the roles played by glia in the nervous system remain largely mysterious. Several observations suggest that glia could influence the shapes of neuronal receptive endings. Electron-microscopy reconstructions demonstrate that glia and glia-like cells associate with most excitatory synapses in the cerebellum and the hippocampus (Spacek, 1985; Ventura and Harris, 1999). Similarly, the endings of diverse sensory cells are ensheathed by glia (Shaham, 2010). The proximity of receptive endings and glial processes might reflect more dynamic interactions between these cellular protrusions. For example, in the cerebellum, Bergmann glia extend and retract processes in concert with the emergence and regression of Purkinje cell dendritic spines (Lippman et al., 2008). Similarly, during lactation in female rats the processes of hypothalamic astrocytic glia retract, and this is accompanied by synaptic remodeling of the glia-ensheathed supraoptic nucleus (SON) neurons (Theodosis and Poulain, 1993).

Laboratory of Developmental Genetics, The Rockefeller University, 1230 York Avenue, New York, NY 10065 USA.

*Author for correspondence (shaham@rockefeller.edu)

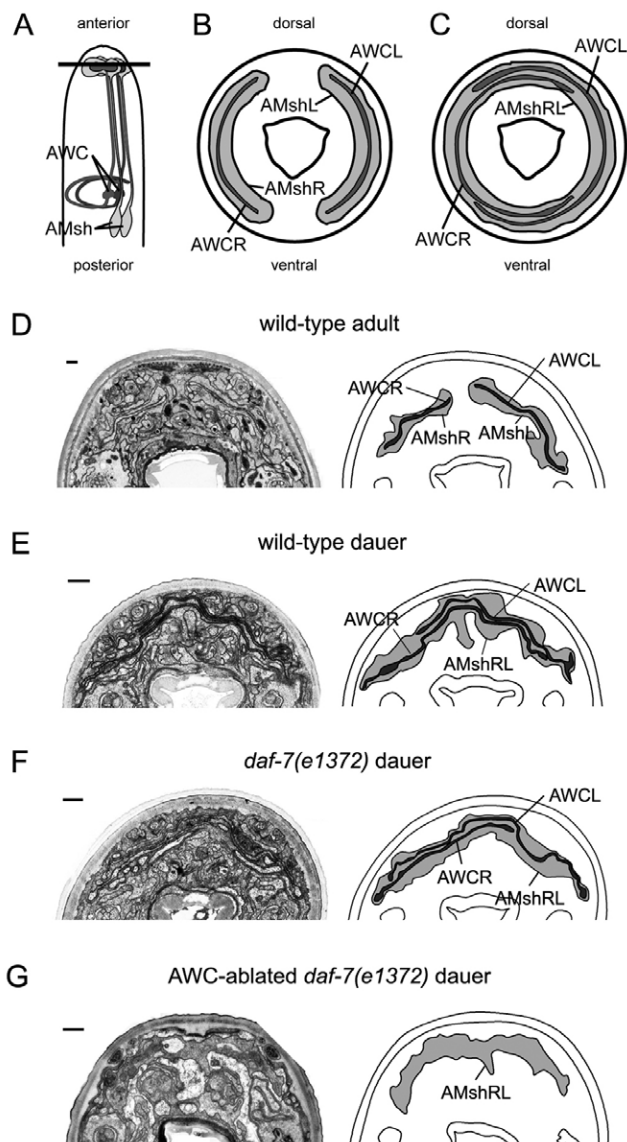


Fig. 1. AWC neuron receptive endings and amphid sheath (AMsh) glia remodel in dauer animals. (A–C) Schematics of amphid remodeling in *C. elegans* dauer larvae. (A) Schematic of the head of the animal, showing the two bilateral AMsh glia and AWC sensory neurons. The horizontal line indicates the position of the transverse sections shown in B and C. (B,C) Sections through the nose tip showing the relative positions of the AWC neuron receptive endings and the ensheathing AMsh glia in non-dauer (B) and dauer (C) animals. AMsh glia fusion can occur on either the ventral or dorsal side (see also Albert and Riddle, 1983). Not to scale. (D–F) Representative electron micrographs (EM) and schematic outlines of amphid sensory organs in non-dauer wild-type adults (D), wild-type dauers induced by starvation (E) and *daf-7(e1372)* dauers (F). Scale bars: 5 μ m. Dorsal is up. (G) EM and schematic outline of the amphid sensory organs of a *daf-7(e1372)*; *AWC::yfp (oys45)* dauer, in which both AWC neurons were ablated in the first larval stage. AMsh glia fusion was scored prior to EM analysis by assaying for glial cytoplasmic mixing (see Fig. 2A). In all schematics, left and right AWC (AWCL/R; dark shading) and AMsh glia (AMshL/R; light shading) are indicated.

Mutations in glial ephrin A3 can alter dendritic spine morphology (Carmona et al., 2009; Murai et al., 2003), and ablation of glia in *C. elegans* can affect the maintenance of sensory

receptive ending shapes (Bacaj et al., 2008), suggesting that, at least in some cases, glia are required to set up receptive ending morphology.

Some glia express neurotransmitter receptors (Porter and McCarthy, 1996) and, in the case of visual cortex astrocytes, exhibit tuning responses similar to those of nearby neurons (Porter and McCarthy, 1996; Schummers et al., 2008). Thus, glia possess machinery to gauge the environment surrounding receptive endings. Together, these various observations raise the intriguing but speculative possibility that extracellular cues received by glia might promote their shape changes, which in turn could affect the shapes of neurons.

Here, we demonstrate that remodeling of *C. elegans* AMsh glia in response to dauer signaling is required for proper morphological changes of the AWC sensory neuron receptive endings in dauers. Remodeling of AMsh glia requires the AFF-1 fusogen, the OTD/OTX transcription factor TTX-1, and probably also its direct target gene, the VEGFR-related protein VER-1. *ver-1* expression is induced by dauer entry and also by high temperature, a dauer stimulus. Our results suggest that glia can play key roles in delimiting changes in neuronal receptive-ending morphology in response to external cues.

MATERIALS AND METHODS

Strains

C. elegans were cultivated using standard methods (Brenner, 1974). The wild-type strain was Bristol (N2). Alleles used were *tax-2(p691)*, *lin-11(n389, n566)*, *che-13(e1805)*, *daf-16(mu86)*, *ire-1(zc14)*, *dac-1(gk211)*, *tax-4(p678)*, *unc-86(e1416, n846)*, *daf-7(e1372)*, *daf-2(m41)*, *osm-9(ky10)*, *ttx-1(p767, oy26)*, *pkc-1(nj1, nj3, nj4)*, *osm-6(p811)*, *ceh-14(ch3)*, *pkc-2(ok328)*, *ttx-3(ks5, mg158)*, *ceh-37(ok642, ok272)*, *ceh-36(ky646)*, *che-2(e1033)*, *dyf-7(ns89, m537)*, *daf-12(m20, m25)* and *lin-15(n765)*. Two *ver-1* alleles were used: *tm1348* and *ok1738*.

ver-1 alleles

The predicted wild-type VER-1 protein is 1083 amino acids and includes an amino-terminal extracellular region, a single transmembrane domain and an intracellular protein kinase domain (Popovici et al., 2002). *tm1348* has a frame-shift deletion that codes for a truncated protein of 267 conserved amino acids lacking the transmembrane and protein kinase domains, and which is followed by an additional non-homologous 21 amino acids (HSPSSETLRSETNSEKFYTFZ). A single base mutation also causes an amino acid change at position 266 (Y to C). *ok1738* has an in-frame deletion (between residues 168 and 417) removing part of the extracellular region.

Transgenic strains

Germline transformations were performed using standard protocols (Mello and Fire, 1995). Co-injection markers were plasmid pRF4 containing the dominant marker *rol-6(su1006)* (Mello et al., 1991), pJM23 containing wild-type *lin-15* (Huang et al., 1994), or fluorescent markers *unc-122* promoter::*dsRed* or *gcy-7* promoter::*gfp*. pSL1180 is an empty cloning vector used to increase the DNA concentration of injection mixtures. *ver-1* promoter::*gfp* and *ttx-1* rescue transgenes were integrated by treating animals carrying extrachromosomal arrays with ultraviolet light in combination with psoralen. The generated strains were backcrossed to N2 more than three times. Arrays and integrants are as designated in the text. *nsEx1391* is F16F9.3 promoter::*gfp* plus pRF4.

Plasmid construction

The initial *ver-1* promoter::*gfp* construct was a gift from R. Roubin and C. Popovici (Molecular Oncology, INSERM, Marseilles). It includes promoter sequence from –2110 to +263 relative to the predicted *ver-1* ATG start site. Additional *ver-1* promoter::*gfp* constructs are as described in the text; promoter regions were ligated into *gfp* vector pPD95.75. *ttx-1*pro1::*dsRed* was made by inserting a 7.5 kb upstream *ttx-1* promoter fragment into *dsRed* vector pEP9. *ttx-1*pro2::*gfp* includes the ~3.5 kb fragment further upstream, followed by the *myo-2* 160 bp minimal promoter to facilitate

expression (Okkema et al., 1993), inserted into pPD95.75. When injected, all lines exhibited green fluorescent protein (GFP) expression in the amphid and phasmid socket cells. Some also had sheath cell expression. Occasionally, weak fluorescence was also observed in other cell types. To create cell-specific rescue constructs, *ttx-1a* and *ttx-1b* splice forms (WormBase release WS206) were PCR amplified from N2-derived cDNA and inserted into heat shock vector pPD49.78. The heat shock promoter was replaced with 2 kb *gcy-8* promoter (AFD expression), 5 kb *vap-1* promoter (AMsh expression), or 2kb F16F9.3 or T02B11.3 promoters, both of which give specific AMsh and PHsh glia expression (Bacaj et al., 2008). T02B11.3 promoter::*ttx-1a* was integrated to generate strain *nsIs219*. The *gcy-8* promoter::*egl-1* construct was created similarly. A double insertion of the *egl-1* cDNA occurred, generating two consecutive *egl-1* cDNAs both running 5' to 3' following the promoter. To create *glia::Otx1* and *glia::Otx2* expression vectors, *ttx-1* cDNA was replaced with mouse *Otx1* and *Otx2* amplified from Marathon-Ready mouse cDNA (Clontech), driven by the F16F9.3 promoter. F16F9.3::*gfp* and F16F9.3::*dsRed* fluorescent reporters were created by inserting 2 kb of F16F9.3 promoter into vectors pPD95.75 and pEP9, respectively. Full-length *eff-1a* and *eff-1* cDNAs were inserted in-frame with *gfp* and following the F16F9.3 promoter to create glia-specific translational fusions. To create GST::TTX-1(HD), the homeodomain of *ttx-1* (lacking the first 154 and last 95 amino acids of the TTX-1A protein) was inserted into GST fusion vector pGEX-5X-1.

Microscopy

ver-1 promoter::*gfp* (*nsIs22*) expression was assayed using a fluorescence dissecting microscope (Leica). Adult hermaphrodites were scored, except as noted. Compound microscope images were taken on an Axioplan II microscope using an AxioCam CCD camera (Zeiss) and analyzed using Axiovision software (Zeiss). Additional images were taken on a Deltavision Image Restoration Microscope (Applied Precision/Olympus) and analyzed using SoftWoRx software (Applied Precision). Dauer animals for electron microscopy were grown at 25°C. These were prepared and sectioned using standard methods (Lundquist et al., 2001). Imaging was performed with an FEI Tecnai G2 Spirit BioTwin transmission electron microscope equipped with a Gatan 4K×4K digital camera.

Dauer selection

Animals were starved and dauers selected by treatment with 1% SDS in M9 solution for 20 minutes. Alternatively, animals carrying the *daf-7(e1372)* mutation were induced to form dauers by incubation at 25°C.

Cytoplasmic mixing assay to score AMsh glia fusion

Adult animals carrying an *nsEx1391* (AMsh *glia::gfp*) array were picked to plates seeded with OP50 bacteria or bacteria expressing dsRNA, and cultivated at 25°C. L1 and L2 progeny carrying the array in one of the two AMsh glia were picked 24 hours later to freshly seeded plates. Mosaic animals were incubated for 48 hours at 25°C before scoring GFP presence in either one or both AMsh glia. Animals carrying a *daf-7(e1372)* mutation were only scored if they were dauer larvae at the end of the assay period (Fig. 2A).

Thermotaxis assays

A linear thermal gradient from 18°C to 26°C was established across an aluminum surface using two Peltier feedback devices (Ryu and Samuel, 2002). Staged adult animals cultivated on OP50 bacteria at 15°C, 20°C or 25°C were washed in S-basal medium and transferred to the center of a 10-cm square Petri dish containing 12 ml NGM agar. This dish was placed onto the aluminum surface, with a thin layer of glycerol between the dish and aluminum slab. Animals were allowed to disperse for 45 minutes, fixed with chloroform and counted across six bins, from cold to hot. The center third of the assay plate was removed from the analysis as some animals did not disperse. Fifty to a few hundred worms participated in each assay. Results shown are averages of four independent trials.

Electrophoretic mobility-shift assay (EMSA)

Double-stranded probes covering 40 bp of the *ver-1* gene, with the predicted TTX-1 wild-type ATTA core binding sequence at the center, were generated by annealing single-stranded, 5' biotin end-labeled

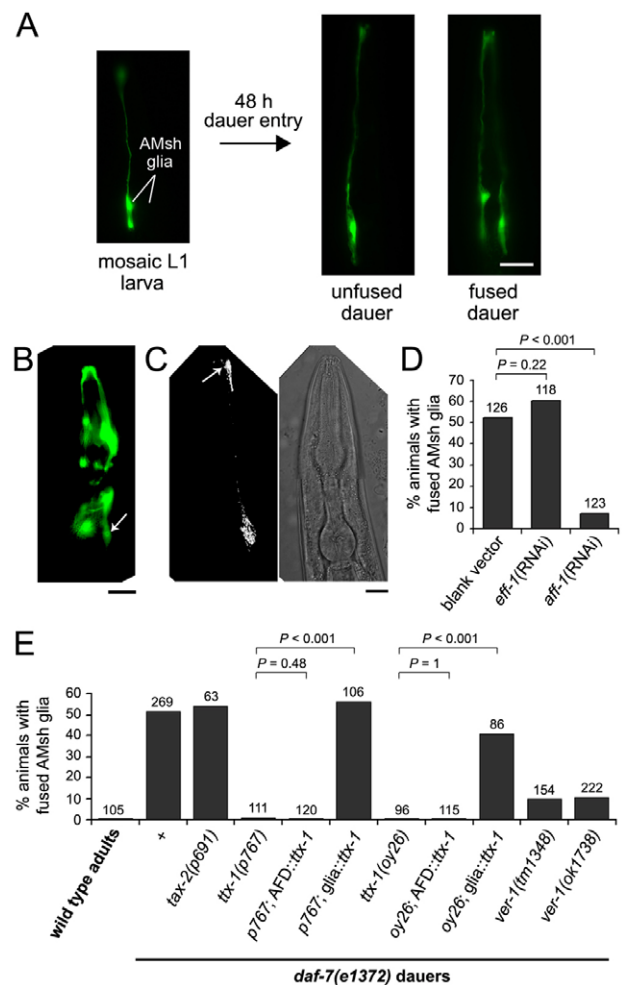


Fig. 2. Scoring amphid sheath (AMsh) glia fusion in *C. elegans* by cytoplasmic mixing. (A) Animals express an AMsh::*gfp* reporter from an unstable extrachromosomal array (*nsEx1391*). First- or second-stage mosaic larvae expressing GFP in one of the two AMsh glia were picked and cultivated for 48 hours at 25°C. If the two AMsh glia fuse at the nose-tip, cytoplasmic mixing occurs and both cells fluoresce. If fusion does not occur, the animals continue to express GFP in only one of the two AMsh glia. Entry into dauer is facilitated by the temperature-sensitive, dauer-constitutive *daf-7(e1372)* allele. Examples of *daf-7(e1372)* dauers where cytoplasmic mixing has and has not occurred are shown. Scale bar: 20 μ m. (B) Fluorescence image of a wild-type adult animal carrying an *aff-1* promoter::*gfp* transgene (*hyEx167*). Arrow indicates AMsh glia cell body. Scale bar: 20 μ m. (C) Fluorescence (left) and differential interference contrast (right) images showing localization of an AFF-1::GFP fusion protein, expressed under an AMsh glia promoter (*nsEx2727*), to the nose-tip (arrow). Punctal cell body expression is also seen. Scale bar: 15 μ m. (D) Percentage of *daf-7(e1372)* dauer animals treated with *eff-1* and *aff-1* RNAi with fused AMsh glia as assayed by cytoplasmic mixing. (E) Percentage of animals with fused AMsh glia as scored by cytoplasmic mixing. Strains carrying a *daf-7(e1372)* mutation are as indicated. Number of animals examined (*n*) is above each column. *P* values were calculated using χ^2 test or Fisher's exact test. Transgenes expressing cell-specific *ttx-1* are *nsIs99* (AFD::*ttx-1*) and *nsIs219* (glia::*ttx-1*). The longest *ttx-1* splice form, *ttx-1a*, was used (see Table 1). In all images, anterior is up.

oligonucleotides. GST::TTX-1(homeodomain) and GST control protein (pGEX-5X-1 empty vector) were induced and purified from BL21(DE3) cells using the Bulk GST Purification Module (GE Healthcare). Binding

reactions were performed using the LightShift Chemiluminescent EMSA Kit (Pierce). Reaction conditions included 400 ng of GST::TTX-1(HD) fusion protein, 1× binding buffer, 2.5% glycerol, 5 mM MgCl₂, 1 μg poly (dI-dC), 0.05% NP-40 and 20 fmol of biotin-labeled DNA probe. GST control protein was added in excess of 400 ng. In competition reactions, a 200-fold molar excess of unlabeled probe was added. Reactions were performed at 20°C for 20 minutes, then run on a 6% polyacrylamide gel in 0.5× TBE buffer. The reactions were transferred to a positively charged nylon membrane and the biotin-labeled DNA was imaged.

RNAi

Plasmids expressing double-stranded RNA (dsRNA) were obtained from the Ahringer library (Fraser et al., 2000). An empty vector was used as the control. RNAi was performed by plating adult *daf-7(e1372)*; *nsEx1391* animals onto RNAi bacteria and allowing them to feed (Timmons and Fire, 1998). Early L1 larvae mosaic for the *nsEx1391* array were re-plated onto fresh RNAi plates and scored 48 hours later.

Cell ablations

AFD thermosensory neurons were ablated by expressing the BH3-only cell death gene *egl-1* (Conradt and Horvitz, 1998) using an AFD-specific promoter (*nsEx755*). AFD ablation was determined by loss of expression of an AFD::*gfp* reporter (*oyIs17*). Thirty-three percent of amphids expressed AFD::*gfp* when carrying *nsEx755*, whereas in a *ced-3(n717)* caspase mutant background, all amphids expressed AFD::*gfp* (both *n*=100), demonstrating that EGL-1 kills AFD. Laser ablations of AWC were performed as described (Bargmann and Avery, 1995) in L1 larvae expressing yellow fluorescent protein (YFP) in AWC (*oyIs45*). Ablation was confirmed by YFP loss.

Statistics

To calculate the significance of *ttx-1* mutant animals showing defects in AWC remodeling by electron microscopy (EM), we proceeded as follows. AMsh glia fusion could occur on either dorsal or ventral sides, or both. By GFP transfer, 50% of *daf-7* mutant dauers fail to exhibit either dorsal or ventral fusion. Thus, if *Q* is the frequency of fusion dorsally or ventrally in a dauer population, then $(1-Q)^2=0.5$, and $Q=0.293$. Therefore, for any six animals without AWC overlap, the probability, *P*, of not having fusion at all is $P=(1-Q)^{12}=0.707^{12}=0.0156$. The same values of *P* are obtained even if *Q* is different between dorsal and ventral sides.

RESULTS

Loss of *daf-7* promotes dauer remodeling of AWC neurons

To characterize remodeling of AWC neuron sensory receptive endings, we examined dauer animals by electron microscopy (EM) serial reconstructions (Albert and Riddle, 1983). We found that in two of three animals examined, AWC receptive endings overlapped extensively. By contrast, no overlap was evident in non-dauer adults (*n*=6) (Fig. 1D,E). These results demonstrate that AWC remodeling occurs in some but not all dauers.

Remodeling of AWC neurons could occur as a direct response to dauer pheromone, or might be a consequence of downstream systemic changes induced by pheromone. To distinguish between these possibilities, we examined animals carrying a temperature-sensitive mutation in the *daf-7* gene (Ren et al., 1996). *daf-7* encodes a TGF-β protein thought to function downstream of pheromone reception, and probably acts to inhibit expression of the dauer program by binding to the DAF-1/DAF-4 TGF-β receptor complex that is expressed on the surfaces of many cells (Estevez et al., 1993; Georgi et al., 1990; Riddle et al., 1981). We found that AWC remodeling still occurred in *daf-7(e1372ts)* animals induced to enter dauer at 25°C. Specifically, two out of three *daf-7(e1372)* dauers examined by EM showed overlap of AWC receptive endings (Fig. 1F; see Fig. S1 in the supplementary material), suggesting that remodeling of AWC is a downstream

consequence of pheromone signaling. These results also demonstrate that *daf-7* mutants are a suitable inducible setting in which to study AWC remodeling.

AMsh glia fusion is dependent on AFF-1 and is not reversible

To probe the extent of AMsh glia remodeling in dauers and to describe the process quantitatively, we developed a fluorescence assay to monitor AMsh glia fusion. First- or second-stage *daf-7(e1372)* larvae expressing an AMsh glia::*gfp* reporter from an unstable extrachromosomal array (*nsEx1391*, F16F9.3 promoter::*gfp*) were selected for mosaic expression of GFP in only one of the two glial cells. These animals were then cultivated for 48 hours at 25°C to induce dauer entry. The presence of GFP in both glial cells in dauers was taken as evidence of cytoplasmic mixing between the cells, indicative of fusion (Fig. 2A).

Four control studies suggest that our assay faithfully reports cell fusion occurrences. First, two independent chromosomally integrated transgenes expressing a fluorescent reporter protein under the F16F9.3 promoter (*nsIs142* and *nsIs143*) were constitutively expressed in both AMsh glia (*n*=100 animals for each line), supporting the notion that single-cell expression of the AMsh glia::*gfp* (*nsEx1391*) reporter is a result of mosaicism of the extrachromosomal array, and not asymmetric reporter expression. Second, we tested whether the presence of GFP in both AMsh glia required molecular mediators of cell fusion. Two *C. elegans* genes, *eff-1* and *aff-1*, encode fusogens required for somatic cell fusion in the animal (Mohler et al., 2002; Sapir et al., 2007). We found that both genes were expressed in AMsh glia (Fig. 2B; see Fig. S2A in the supplementary material) (Mohler et al., 2002; Sapir et al., 2007) and localized to the apical region that undergoes fusion in dauers (Fig. 1, Fig. 2C; see Fig. S2B in the supplementary material). Furthermore, glia fusion was markedly reduced in *aff-1*(RNAi) dauers (Fig. 2D), demonstrating an important role for AFF-1 in glia remodeling. Third, EM serial reconstructions confirmed that glia remained unfused in dauer animals expressing GFP in only one AMsh glial cell, whereas dauers expressing GFP in both AMsh glia had fused glia (see below; also data not shown). Fourth, complete GFP transfer in mosaic animals observed over time took less than 2 hours (*n*=17) and fluorescence was initially more intense at the nose tip (see Fig. S3 in the supplementary material), consistent with cell fusion.

Using our validated assay, and consistent with our EM studies, we found that AMsh glia fusion was never observed in wild-type, non-dauer adult animals, whereas 51% of animals induced to enter dauer by the *daf-7(e1372)* mutation had fused AMsh glia (Fig. 2E; $P<0.001$, χ^2 test). To address whether remodeling of AMsh glia was reversible upon dauer exit, we examined post-dauer *daf-7(e1372)* adult animals recovered by cultivation of dauers at 15°C for 7 days. GFP perdures in AMsh glia for two days or less (Perens and Shaham, 2005); however, we found equal GFP fluorescence in both glial cells (see Fig. S2C in the supplementary material; *n*=44). Furthermore, EM serial reconstruction of a single wild-type 2-day post-dauer adult revealed fused AMsh glia (see Fig. S2D in the supplementary material). Together, these results suggest that remodeling induces a permanent change in AMsh glia architecture.

AMsh glia remodeling is independent of AWC expansion

In all dauers and normally developed adults that we examined by EM serial reconstructions, regardless of genotype, we found that overlap of AWC sensory receptive endings correlated with AMsh

glia expansion and fusion (8 and 19 animals examined with and without AWC overlap, respectively; Fig. 1E,F; see also below). In one *daf-7(e1372)* dauer, glia expanded to allow overlap of the bilateral AWC receptive endings, but did not fuse (see Fig. S1 in the supplementary material). These observations suggested to us that the remodeling of AMsh glia, with or without fusion, might be required to define a compartment into which the AWC receptive endings expand in dauers.

Changes in glial architecture to accommodate the remodeling of AWC receptive endings could be induced by the AWC neuron. Alternatively, glia might independently define a compartment that limits the extent of AWC expansion. To distinguish between these possibilities, we ablated the two AWC neurons using a laser microbeam in first-stage *daf-7(e1372)* larvae that were mosaic for AMsh glia::*gfp* expression and that expressed an AWC promoter::*yfp* reporter (*oyIs45*). Ablated animals were then induced to become dauers by incubation at 25°C for 48 hours, and glial fusion was monitored using the cytoplasmic mixing assay. We found that mock-ablated animals had a high rate of fusion (89%; $n=36$), perhaps a result of the strain background. Importantly, in animals where both AWC neurons were ablated, we saw no significant decrease in glial cell fusion (81%; $n=26$; $P=0.47$, Fisher's exact test). EM serial reconstructions of ablated animals confirmed both the degradation of the AWC receptive endings and the remodeling of the glia in the absence of AWC expansion (Fig. 1G; $n=2$).

These results suggest that in response to external dauer signals the AMsh glia, independently of AWC neurons, define a compartment that delimits AWC receptive ending expansion.

ttx-1 is required in AMsh glia for glia remodeling

The observation that glia can remodel in the absence of AWC neurons suggests that active processes within AMsh glia might be required to promote glia remodeling and that interference with these processes should lead to defects in AWC sensory receptive ending shape. To test this prediction and to begin to characterize the molecular basis for glia remodeling, we sought fully penetrant mutants in which glia remodeling was blocked. Importantly, because our previous studies indicated that AMsh glia are required for maintaining AWC receptive ending shape (Bacaj et al., 2008), we aimed to identify mutants that specifically disrupt glia remodeling in dauers, but in which glial shape was unperturbed in non-dauer animals. *aff-1* was unsuitable for such an analysis: RNAi knockdown of *aff-1* did not have a fully penetrant defect in glial remodeling, and *aff-1* genetic lesions had morphological abnormalities in the AMsh glia and other tissues (data not shown) (Sapir et al., 2007).

In the course of our studies, we found that transcription of the AMsh glia gene *ver-1* was temperature dependent. We therefore examined the effect of the thermotaxis gene *ttx-1*, encoding an OTD/OTX transcription factor (Satterlee et al., 2001), on *ver-1* expression (see below) and glial fusion. As shown in Fig. 2E, AMsh glia fusion failed to occur in almost all *daf-7(e1372)*; *ttx-1(p767)* and *daf-7(e1372)*; *ttx-1(oy26)* double-mutant dauer animals scored using the cytoplasmic mixing assay. Thus, *ttx-1* might be a component of the glial remodeling machinery, and *ttx-1* mutants might provide a suitable genetic background in which to test the effects of AMsh glia remodeling on AWC neuron shape changes.

However, previous studies suggested that *ttx-1* is expressed specifically in the AFD thermosensory neurons of *C. elegans*. Animals carrying *ttx-1* promoter::*gfp* transgenes express GFP in

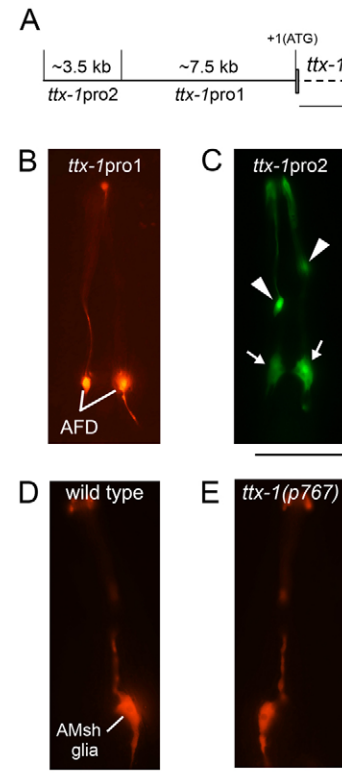


Fig. 3. *ttx-1* is expressed in glia. (A) Schematic of the *ttx-1* promoter. The ATG start codon and first exon (narrow vertical box) are shown, as well as 11 kb of upstream sequence (solid horizontal line). The *ttx-1*pro1 region includes the 7.5 kb sequence upstream and adjacent to the *ttx-1* start site. The *ttx-1*pro2 region includes the 3.5 kb sequence upstream of *ttx-1*pro1. Scale bar: 2 kb. Dotted horizontal line represents part of the first intron. (B) Fluorescence image of an adult animal carrying a transgene containing the *ttx-1*pro1 sequence fused to *dsRed* (*nsEx1320*). Fluorescence is seen in the two AFD thermosensory neurons. (C) Fluorescence image of an animal carrying a transgene containing the *ttx-1*pro2 sequence fused to *gfp* (*nsEx1942*). Reporter expression is evident in the amphid sheath (AMsh; arrows) and amphid socket (arrowheads) glia. (D,E) Representative fluorescence images of *vap-1* promoter::*dsRed* (*nsIs53*) expression within an AMsh glial cell at 20°C in wild-type (D) and *ttx-1(p767)* mutant (E) adults. Exposure time, 250 ms. Scale bars: 50 μ m. In all images, anterior is up.

AFD (Satterlee et al., 2001), and the AFD sensory receptive endings in *ttx-1* mutants lack their wild-type microvilli-like protrusions (Perkins et al., 1986). Furthermore, *ttx-1* mutants have defects in thermotaxis, an AFD-dependent behavior in which animals placed in a thermal gradient seek the temperature at which they were reared (Hedgecock and Russell, 1975; Mori and Ohshima, 1995). *ttx-1* might, therefore, act in AFD to drive AMsh glia fusion in dauers. To test this possibility, we blocked activity in a number of amphid sensory neurons, including AFD, using a mutation in the *tax-2* gene, which encodes a subunit of a cyclic nucleotide gated channel required for thermotaxis and other sensory functions (Coburn and Bargmann, 1996; Komatsu et al., 1996). We observed no defect in the fusion of AMsh glia in *tax-2(p691)* mutants (Fig. 2E; $P=0.70$, χ^2 test), suggesting that sensory signaling in AFD was unlikely to be important for glia remodeling. These results suggested the possibility that *ttx-1* might act in AMsh glia to promote their remodeling in addition to its previously described roles in AFD.

To test this idea, we examined expression of transgenes containing *ttx-1* regulatory sequences fused to sequences encoding fluorescent reporter proteins. As shown in Fig. 3, a 7.5 kb sequence immediately upstream of the *ttx-1* transcription start site drives reporter expression in AFD, consistent with previous observations (Satterlee et al., 2001). By contrast, a 3.5 kb sequence further upstream drives expression in AMsh and phasmid sheath (PHsh) glia, as well as in associated socket glia (Fig. 3A,C; data not shown). The PHsh glia are associated with the phasmid sensory organ in the tail. Furthermore, by driving *ttx-1* cDNA under cell-specific promoters (see Materials and methods), we observed that, although expression of *ttx-1* in AFD was sufficient to confer wild-type AFD sensory ending morphology and thermotaxis to *ttx-1* mutants (see Fig. S4A-C,F-H in the supplementary material) (Satterlee et al., 2001), it did not rescue the AMsh glia fusion defect in dauer animals (Fig. 2E). Restoring *ttx-1* in AMsh glia, however, rescued AMsh glia fusion (Fig. 2E) but not thermotaxis or AFD morphology (see Fig. S4A,D,E,I in the supplementary material). These results demonstrate that *ttx-1* has separable, cell-autonomous roles in the AFD thermosensory neurons and the AMsh glia.

To determine whether *ttx-1* was generally required for AMsh glia shape maintenance, we examined the morphology of these cells in non-dauer animals. We found no defects in glial shape. Furthermore, expression of constitutively expressed glial genes was affected weakly or not at all by mutations in *ttx-1* (Fig. 3D,E; data not shown). In addition, an *aff-1* promoter::*gfp* reporter (*hyEx167*) showed GFP expression in AMsh glia of both wild type and *ttx-1* mutants [86% of wild-type animals expressed GFP in AMsh glia, compared with 93% of *ttx-1(p767)* mutants; $n > 40$ for each genotype], suggesting that *ttx-1* probably affects glia remodeling and fusion through the transcriptional regulation of genes other than *aff-1*.

Our data show that *ttx-1* has specific cell-autonomous roles in AMsh glia, supporting the idea that active glia-intrinsic processes promote glia remodeling. These results also suggest that animals lacking *ttx-1* function provide a suitable setting in which to test the effects of AMsh glia on AWC neuron remodeling.

Proper remodeling of AWC neurons requires glia

To address whether remodeling of AWC receptive endings in dauer animals depends on remodeling of AMsh glia, we examined EM serial sections of *ttx-1* mutants. We first noted that *ttx-1(p767)* starvation-induced dauers as well as *ttx-1(p767); daf-7(e1372)* dauers did indeed fail to show AMsh glia fusion (Fig. 4A,B; $n=6$), verifying the results of our cytoplasmic mixing assay. Importantly, in these same animals, AWC receptive endings did not overlap extensively (Fig. 4A,B; $n=6$, $P < 0.016$). Furthermore, animals in which AMsh glia fusion was rescued by restoring *ttx-1* expression in these cells displayed a wild-type pattern of AWC overlap by EM (Fig. 4C; $n=2$). Interestingly, in two out of the six *ttx-1* mutants we examined, AWC appeared to have expanded but, instead of projecting circumferentially around the nose as was always observed when AWC expanded in wild-type dauers, folded back on itself (see Fig. S5 in the supplementary material; see Discussion).

The AWC ablation and *ttx-1* studies demonstrate that AMsh glia respond to dauer signals independently of AWC to define a compartment confining AWC receptive endings, and that defects in glial compartment plasticity lead to defects in the morphology of AWC receptive endings.

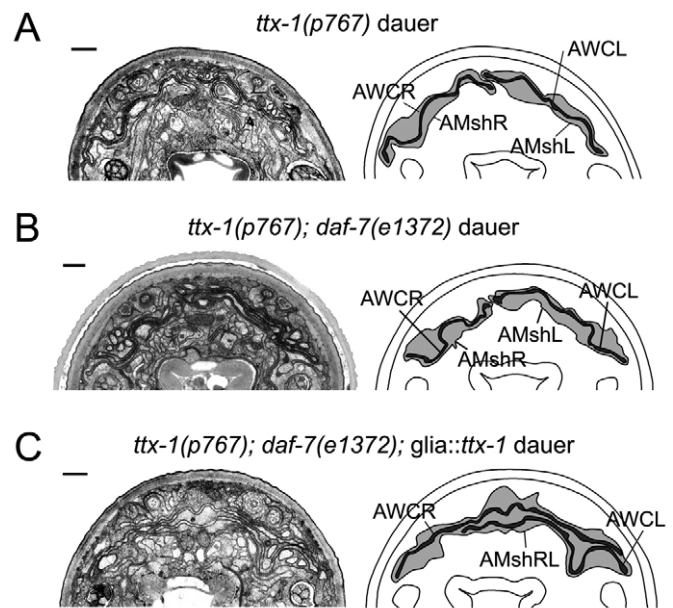


Fig. 4. *ttx-1* is required for remodeling of amphid sheath (AMsh) glia in *C. elegans*. (A-C) Representative electron micrographs (EM) and schematic outlines of amphid sensory organs in *ttx-1(p767)* dauers induced by starvation (A), *ttx-1(p767); daf-7(e1372)* dauers (B) and *ttx-1(p767); daf-7(e1372); glia::ttx1(nsls219)* dauers with fused AMsh glia as assayed by cytoplasmic mixing prior to EM analysis (C). Left and right AWC (AWCL/R; dark shading) and AMsh cells (AMshL/R; light shading) are indicated. Scale bars: 5 μ m. Dorsal is up.

ttx-1 might promote AMsh glia remodeling by inducing *ver-1* expression

Although morphological plasticity of glia has been demonstrated in some settings, neither the effects of glial shape changes on neuronal shape, nor the molecular mechanism promoting glial shape changes has been described in any animal. To elaborate further the mechanism by which *ttx-1* promotes the remodeling of AMsh glia, we turned our attention to the gene *ver-1*. *ver-1* encodes a receptor tyrosine kinase (RTK) with similarities to the mammalian vascular endothelial growth factor receptor (VEGFR), and was previously reported to be expressed in AMsh and PHsh glia (Popovici et al., 2002). Interestingly, we found that at 15°C, wild-type dauers induced by starvation strongly expressed a *ver-1* promoter::*gfp* reporter in AMsh and PHsh glia (Fig. 5A,C) (Popovici et al., 2002). However, only very weak expression of *ver-1* was detected in non-dauer adults raised under the same temperature conditions (Fig. 5B,D). Thus, *C. elegans* AMsh glia respond to dauer signals by modifying gene expression concomitantly with induction of remodeling.

The induction of *ver-1* expression in dauers suggested that this gene might be involved in remodeling AMsh glia. To test this idea, we examined two strains carrying different deletions of the *ver-1* locus (see Materials and methods) using our fluorescence fusion assay. As shown in Fig. 2E, both strains displayed significantly reduced AMsh glia fusion ($P < 0.001$, χ^2 tests; perhaps for technical reasons, we have not been able to obtain transgenic rescue of the mutants). Furthermore, we found that expression of *ver-1* in glia was dependent on functional *ttx-1*, as two independent *ttx-1* alleles greatly reduced *ver-1* promoter::*gfp* expression in dauers (Fig. 5E). To determine how TTX-1 regulates *ver-1* expression, we performed deletion studies of the *ver-1* promoter with the aim of identifying

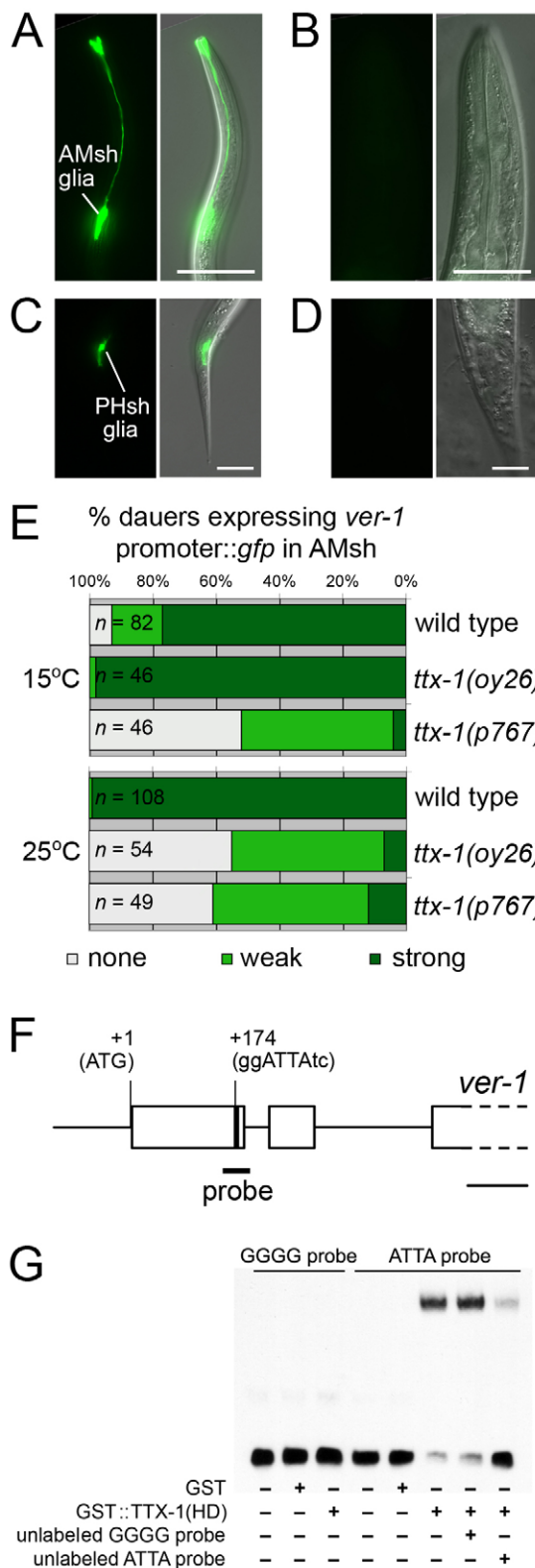


Fig. 5. Dauer-induced expression of *ver-1* is dependent on *ttx-1*. (A,B) Representative fluorescence images (left), and differential interference contrast and fluorescence merged images (right) of the two amphid sheath (AMsh) glial cells of a wild-type dauer induced by starvation at 15°C (A), and in a non-dauer adult animal at 15°C (B). Exposure time for *ver-1* promoter::*gfp* was 800 ms. Scale bars: 50 μm. Anterior is up. (C,D) As in (A,B), except showing *ver-1* promoter::*gfp* (*nsls22*) expression in the phasmid sheath (PHsh) glia. Exposure time was 200 ms. Scale bars: 50 μm. Anterior is up. (E) Expression of a *ver-1* promoter::*gfp* transgene (*nsls22*) in AMsh glia of wild-type, *ttx-1(oy26)* and *ttx-1(p767)* dauers at 15°C and 25°C. GFP expression is scored as either strong (dark green), weak (green) or absent (white). The *ttx-1(oy26)* allele blocks *ver-1* expression in dauers at 25°C but not at 15°C. (F) Schematic showing part of the predicted *ver-1* gene and promoter. Wormbase-predicted exons are shown as boxes, non-coding regions as a solid horizontal line. The ATG start codon, putative TTX-1 binding site (ggATTAtc; core binding residues in capital letters), and location of the 40-bp probe used in G are shown. Scale bar: 100 bp. (G) Electrophoretic mobility-shift assay showing binding of either a GST control or a purified GST::TTX-1 homeodomain fusion protein to a wild-type (ATTA) or mutant (GGGG) 40 bp biotin-labeled probe from the *ver-1* promoter. Competitor, unlabeled wild-type or mutant probes were added in 200-fold excess.

that *ttx-1* might directly regulate *ver-1*. Indeed, a 40 bp oligonucleotide containing this sequence bound a GST::TTX-1 homeodomain fusion protein, and alteration of the core nucleotides of the putative binding site from GGATTATC to GGGGGGTC abolished both in vitro binding (Fig. 5F,G) and in vivo expression of a *ver-1* promoter::*gfp* transgene (see Table S1 in the supplementary material). Thus, *ver-1* is probably a direct TTX-1 target.

Taken together, these results suggest that *ttx-1* might act to regulate AMsh glia fusion in dauer animals in part by promoting *ver-1* expression.

***ver-1* exhibits temperature-dependent expression in dauers and non-dauers**

Although *ver-1* expression was strongly induced by dauer entry, we also noticed induction of expression by high ambient temperature in non-dauer animals. Over a temperature range of 15-25°C, adult animals exhibited a graded increase in *ver-1* promoter::*gfp* expression intensity (Fig. 6A; data not shown). The increase in expression was not a general transcriptional response, as reporters for three other glial genes demonstrated only mild temperature effects and were not upregulated by dauer entry (see Fig. S6 in the supplementary material). Furthermore, neither the heat-shock nor the unfolded protein response pathways affected *ver-1* expression (see Table S2 in the supplementary material; data not shown), indicating that the expression pattern observed was not a result of a general stress response.

The induction of *ver-1* expression by temperature was, however, dependent on *ttx-1*, as animals containing *ttx-1* mutations failed to express the *ver-1* promoter::*gfp* reporter at high temperatures (Fig. 6B). Restoring *ttx-1* specifically in glia rescued temperature-dependent *ver-1* expression, whereas restoring *ttx-1* in AFD neurons did not (Table 1). In addition, the same promoter region and TTX-1 binding site required for expression of *ver-1* in dauers were required for temperature-dependent expression of *ver-1* (see Table S1 in the supplementary material).

a minimal interval required for expression of the gene. We identified a ~100 bp interval required for *ver-1* expression in dauers (see Table S1 in the supplementary material). Within this interval we identified a potential TTX-1 binding site based on similarity to the mammalian Otx2 binding site (Kelley et al., 2000), suggesting

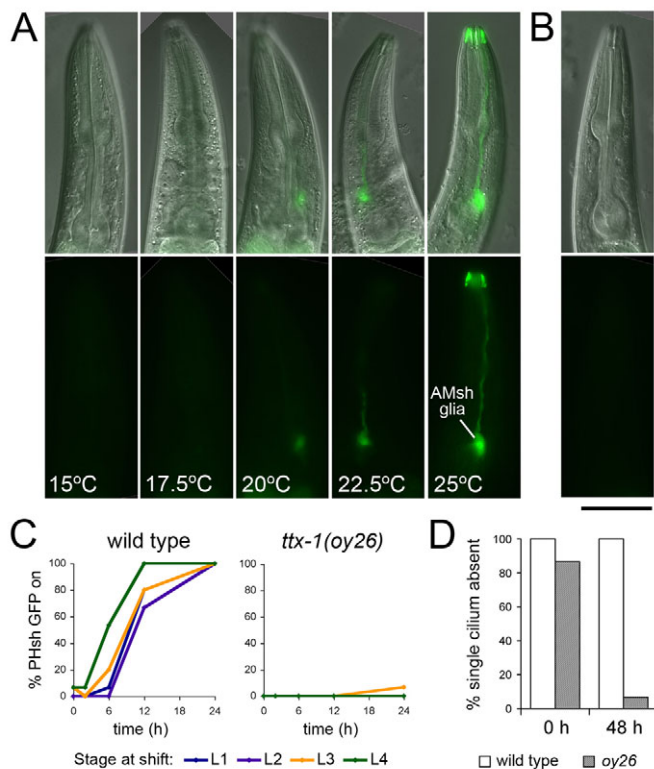


Fig. 6. TTX-1 is required continuously for temperature-dependent expression of *ver-1* in amphid sheath (AMsh) glia and for AFD sensory ending morphology. (A) Representative differential interference contrast (DIC) and fluorescence merged images (top), and fluorescence only images (below) of *ver-1* promoter::*gfp* (*nsls22*) expression in one of the two AMsh glial cells of wild-type animals at 15–25°C. (B) DIC and fluorescence merged (top), and fluorescence only (below) images of *ver-1* promoter::*gfp* expression in a *ttx-1(p767)* mutant adult at 25°C. (C) Percentage of wild-type and temperature-sensitive *ttx-1(oy26)* mutant larvae (L1–L4 stages) expressing *ver-1* promoter::*gfp* in phasmid sheath (PHsh) glia over time (hours, h) following a temperature shift from 15°C to 25°C ($n=15$ for each data point). *ver-1* promoter::*gfp* expression in AMsh glia showed a similar trend; however, PHsh glial GFP fluorescence was greater (data not shown). (D) The percentage of wild-type and *ttx-1(oy26)* L4 animals in which AFD dendrite endings do not exhibit an aberrant single cilium morphology at 0 and 48 hours (h) following a temperature shift from 15°C to 25°C. In some animals possessing a single aberrant cilium, some microvilli were still observable at the base of the cilium. Results are comparable with second- and third-stage larvae (data not shown). $n=15$ for both genotypes. A *gcy-8* promoter::*gfp* transgene (*oyls17*) was used to visualize the AFD neurons. For a description of the effect of the *ttx-1(oy26)* allele on AFD morphology at different temperatures, see Fig. S7 in the supplementary material. In A and B, exposure time for *ver-1* promoter::*gfp* was 800 ms. Scale bar: 50 μ m. In all images, anterior is up.

Otx2 is expressed in glia-like cells in olfactory and vomeronasal organ epithelia (Mallamaci et al., 1996), suggesting that the functions of this family of proteins in sense organs might be widely conserved. We found that expression of *Otx2*, but not *Otx1*, robustly rescued the defects in *ver-1* expression at 25°C of *ttx-1* mutants (Table 1). These results are consistent with the notion that both proteins might have similar functions in their natural settings.

Interestingly, restoring *ttx-1* to adult mutant animals using a heat-inducible promoter rescued *ver-1* expression at 25°C (see Table S3 in the supplementary material). In addition, we found that the *ttx-1(oy26)* allele was temperature-sensitive (Fig. 5E; see Fig. S7 in the supplementary material), and that shifting *ttx-1(oy26)* animals reared at 15°C (the permissive temperature) to 25°C (the restrictive temperature) at any larval stage abrogated *ver-1* promoter::*gfp* expression in glia (Fig. 6C), suggesting that *ttx-1* is continuously required for *ver-1* expression at 25°C. Strikingly, we also observed a continuous requirement for *ttx-1* in maintaining AFD sensory ending morphology: *ttx-1(oy26)* mutants shifted to the non-permissive temperature acquired an aberrant, single elongated cilium (Fig. 6D; see Fig. S7 in the supplementary material). Thus, in both glia and neurons, *ttx-1* functions continuously to control specialized aspects of terminal differentiation.

To determine whether temperature control of *ver-1* expression was mediated by the sensory neurons associated with the AMsh glia, we genetically ablated both thermosensory AFD neurons and observed no defect in *ver-1* expression (Table 1). Likewise, perturbation of all amphid and phasmid sensory neuron signaling activity by mutations in the *tax-2*, *tax-4* and *osm-9* sensory transduction ion channels (Coburn and Bargmann, 1996; Colbert et al., 1997; Komatsu et al., 1996) had little effect on the induction of *ver-1* expression at high temperature (Table 1). Importantly, these mutations also had no effect on *ver-1* expression in dauer animals (Table 1, footnote). Finally, mutations disrupting sensory neuron cilia morphology and/or circuitry, or mutations in dauer-related TGF- β (Ren et al., 1996) or insulin (Kimura et al., 1997) neuroendocrine signaling components, also had minor or no effects on *ver-1* expression at 25°C (see Table S2 in the supplementary material). These observations suggest that AMsh and PHsh glia respond to temperature independently of sensory neuron input, and that the induction of *ver-1* expression in dauers and at high temperature is mediated, at least in part, by similar programs.

To assess whether increased *ver-1* expression was sufficient to drive AMsh glia remodeling, we examined non-dauer adults raised at 25°C for fusion of AMsh glia. We found that fusion does not occur in these animals (Fig. 2E; see above), even though *ver-1* is highly expressed, suggesting that dauer entry provides additional necessary conditions for AMsh glia remodeling.

High ambient temperature is one of the environmental stressors that regulate dauer entry (Golden and Riddle, 1984), raising the possibility that increased expression of *ver-1* at high temperatures might facilitate AMsh glia remodeling. However, robust expression of *ver-1* is still detected in dauers raised at 15°C, confounding a functional analysis of the effects of temperature on the remodeling of these glia. Nonetheless, we still observed a temperature dependence of *ver-1* expression in dauers raised at different temperatures (see Table S1 in the supplementary material). Thus, although temperature and dauer signals both require TTX-1 to induce *ver-1* expression, these signals must also converge independently on the *ver-1* promoter to induce expression in dauer animals. These results raise the speculative possibility that temperature, in addition to dauer cues, might play a modulatory role in remodeling of AMsh glia.

DISCUSSION

Glia as regulators of neuronal receptive ending shape

The results described here show that the extent of remodeling of a glial compartment in *C. elegans* dauers restricts the shape of remodeled AWC receptive endings: when *ttx-1* function in glia is

Table 1. TTX-1 acts in glia, and not AFD, to control temperature-dependent *ver-1* expression

Genotype*	<i>ver-1</i> expression 15°C			<i>ver-1</i> expression 25°C		
	% PHsh on	% AMsh on	<i>n</i>	% PHsh on	% AMsh on	<i>n</i>
wild type	6	0	80	100	93	80
<i>ttx-1(p767)</i>	0	0	70	0	0	70
<i>ttx-1(p767); AFD::ttx-1</i>	0	0	25	0	0	23
<i>ttx-1(p767); AMsh::ttx-1[†]</i>	0	0	25	0	50	22
<i>ttx-1(p767); AM+PHsh::ttx-1</i>	30	7	30	87	97	30
<i>ttx-1(oy26)</i>	0	0	30	0	0	30
<i>ttx-1(oy26); AFD::ttx-1</i>	0	0	25	0	0	21
<i>ttx-1(oy26); AMsh::ttx-1[†]</i>	0	4	25	0	48	23
<i>ttx-1(oy26); AM+PHsh::ttx-1</i>	57	7	30	83	93	25
<i>ttx-1(p767); glia::Otx1[‡]</i>	0	0	40	0	8	40
<i>ttx-1(p767); glia::Otx2</i>	0	0	40	45	100	40
AFD genetic ablation [§]	8	0	40	100	93	40
<i>tax-2(p691)</i>	0	0	41	100	88	50
<i>tax-4(p678)</i>	2	0	46	100	83	76
<i>osm-9(ky10)</i>	3	0	40	100	95	40
<i>tax-2(p691); osm-9(ky10)[¶]</i>	8	0	40	100	90	40

*All strains contained the *ver-1* promoter::*gfp* transgene (*nsIs22*).

[†]That *ttx-1* expression only in AMsh glia rescued *ver-1* expression only in AMsh glia supports a cell autonomous role for *ttx-1*.

[‡]The glia promoter drives expression in both AMsh and PHsh glia.

[§]See Materials and methods.

[¶]The *tax-2(p691); osm-9(ky10)* genotype also failed to affect *ver-1* expression in dauers. 100% of *tax-2(p691); osm-9(ky10)* starvation-induced dauers at 15°C expressed *ver-1* promoter::*gfp* in PHsh and 82% in AMsh, compared with 100% of wild-type dauers in PHsh and 88% in AMsh (*n*=50 for each genotype).

Two *ttx-1* cDNAs, *ttx-1a* and *ttx-1b*, were isolated and gave equivalent rescue. TTX-1A and TTX-1B proteins are identical, except for an additional 53 amino acid residues in TTX-1A. Only *ttx-1a* rescue transgenes are shown. Transgenes were injected at 60 ng/μl of *ttx-1* or *Otx* plasmid, with 60 ng/μl of pRF4. Lines shown are *nsEx899*, *nsEx895*, *nsEx939*, *nsEx897*, *nsEx893*, *nsEx937*, *nsEx1661* and *nsEx1662*, and are representative of others. AMsh, amphid sheath; PHsh, phasmid sheath.

impaired, the AWC sensory protrusions fail to take on their wild-type overlapping appearance. Glia or glia-like cells are intimately associated with sensory receptive endings from *C. elegans* to humans (Shaham, 2010), suggesting that the roles they play in delimiting receptive ending morphological plasticity might be conserved. Furthermore, the many similarities between sensory receptive endings and dendritic spines, which serve as receptive endings for presynaptic neurons (Shaham, 2010), suggest the interesting possibility that glia could be in a position to define compartments that will constrain dendritic spine shape also. Indeed, all dendritic spines examined by EM in the cerebellum are tightly ensheathed by Bergmann glia (Spacek, 1985), and most spines examined by EM in the hippocampus are ensheathed by astrocytes (Ventura and Harris, 1999). Furthermore, Bergmann glia have been shown to affect neuronal receptive ending shapes in the cerebellum (Lippman et al., 2008), and astrocytic glia affect dendritic spine morphology of hippocampal neurons via ephrin-A3/EphA4 signaling (Murai et al., 2003).

At least two possible mechanisms by which the glial compartment can delimit receptive-ending shape are possible. Glia might form an inelastic physical barrier against expansion of neuronal receptive endings. Alternatively, glia might provide specific signals that induce receptive-ending growth or retraction. Although both mechanisms could apply, our finding that in some *ttx-1* mutants AWC attempts to remodel but forms membrane whorls confined to the space defined by the AMsh glia (see Fig. S5 in the supplementary material) is consistent with a physical barrier role for these cells. A similar role for astrocytic glia in remodeling SON neuron synapses in the mammalian hypothalamus has been proposed: the retraction of astrocytic processes from postsynaptic

surfaces might facilitate the increased number of synapses that occur onto a single postsynaptic element during lactation in female rats (Theodosios and Poulain, 1993). In both of these cases, remodeling of the glia could be permissive for neuronal shape changes.

Our studies demonstrate that neuronal remodeling must be tightly coordinated with glia remodeling in dauer animals, predicting the existence of proteins tasked with executing this coordination. That *ver-1* encodes a receptor tyrosine kinase is intriguing, suggesting the speculative possibility that it normally responds to as yet unidentified neuronal cues to promote coordinated glia-neuron remodeling. Expression of *ver-1* in non-dauer animals might serve to prime glia for remodeling, in preparation of pending dauer entry. In addition, *ver-1* expression might represent a neuroprotective or stress response of the glia. Supporting this possibility, the VER-1-related VEGF receptor Flk-1 (also known as VEGFR-2; Kdr – Mouse Genome Informatics) is expressed in neurons and glia of the mammalian hippocampus following nerve injury stress (Wang et al., 2005), and VEGF signaling has neurotrophic and neuroprotective roles in some contexts (Sondell et al., 1999). Furthermore, the predicted *ver-1* kinase domain is similar to kinase domains encoded by the *C. elegans* genes *old-1* and *old-2* (~40% identity), and *old-1* has been implicated in longevity and resistance to environmental insults (Murakami and Johnson, 2001).

The functional outcome of AWC receptive-ending remodeling in dauers is unclear; however, previous studies have correlated AWC sensory ending shape with function (Perkins et al., 1986). It is possible, therefore, that the morphological changes in AWC promote a change in the behavior of the animal. To date, no AWC-

mediated behaviors have been described for dauers. Indeed, in dauer animals the expression of at least one AWC odorant receptor is repressed (Peckol et al., 2001), and the classical AWC-sensed attractants benzaldehyde and isoamylalcohol act instead as repulsive cues (C.P. and S.S., unpublished; data not shown). These observations suggest that assessing the functional consequences of dauer remodeling will require a more thorough description of sensory neuron function and molecular biology in dauers than is presently available.

The receptive endings of the amphid AFD thermosensory neurons might also remodel in dauer animals, as the number of AFD microvilli has been reported to increase upon dauer entry (Albert and Riddle, 1983). Thus, it is possible that AMsh glia play a role in this remodeling process also. However, EM serial reconstructions of young larva and adults from our laboratory demonstrate that adults always possess a larger number of microvilli (Y.L. and S.S., unpublished), suggesting that the increase in microvilli number observed in dauers could also be explained by a constant rate of microvilli addition that is independent of the dauer state. In addition, we are unable to use *ttx-1* mutants to assess the effects of AMsh glia on AFD remodeling, as *ttx-1* also functions within AFD to control morphology.

At excitatory synapses, changes in dendritic spine volume are positively correlated with the extent of presynaptic activity (Feldman, 2009; Holtmaat and Svoboda, 2009), suggesting that extracellular cues are important in driving changes in receptive ending shape. Glia can directly sense extracellular stimuli such as Na⁺ levels (Shimizu et al., 2007), neurotransmitters (Porter and McCarthy, 1996) and perhaps protons (Wang et al., 2008). Our studies demonstrate that the AMsh glia can respond to dauer entry and temperature, both exogenous stimuli, and do so independently of sensory neuron input. Furthermore, at least one gene, *ver-1*, is dynamically regulated by both cues. It is therefore reasonable to speculate that glia sense these stimuli, and in turn modulate their shapes to accommodate morphological changes of nearby neuronal receptive endings.

***ttx-1* regulates cell shape in thermoresponsive cells**

It is not known whether the temperature responses of AFD and AMsh glia are mediated by the same or different sensors. A sensor has not yet been identified in either cell; however, three guanylyl cyclases are important for temperature sensation in AFD, suggesting a possible involvement of a G-protein coupled receptor (Inada et al., 2006). Reporter constructs for these guanylyl cyclases are not expressed in AMsh glia (Inada et al., 2006), suggesting that glia might employ a different sensor. However, it is also possible that these cyclases function permissively in AFD, and do not directly interact with the sensor. In *Arabidopsis*, changes in ambient temperature cause fluctuations in the constituents of nucleosomes (Kumar and Wigge, 2010). Thus, chromatin might act as a direct thermal sensor. Such a sensor is unlikely to be employed in AFD neurons, as it is not compatible with the fast calcium transients observed in AFD neurons following temperature shifts (Kimura et al., 2004). A DNA-bound sensor would, however, be consistent with the kinetics of temperature-induced changes in *ver-1* expression that we observe in glia (see Fig. 6C). If such a sensor exists, TTX-1 would be unlikely to be its temperature sensitive component, as constitutive expression of TTX-1 or its mammalian homolog Otx2, in glia does not perturb temperature sensitivity of *ver-1* expression (Table 1; see Fig. S3 in the supplementary material).

It is of note that *ttx-1* is required for determining the morphology of process endings of both glia (fusion/expansion) and neurons (AFD microvilli). Interestingly, ectopic expression of TTX-1 in non-AFD neurons induces protrusions in these cells (Satterlee et al., 2001). Thus, TTX-1 might have specific roles in regulating cell shape. Furthermore, the role of the protein as a terminal cell fate gene might be limited to thermoresponsive cells, as TTX-1 is required in two seemingly unrelated temperature-dependent processes in *C. elegans*: AFD neuron function and glial *ver-1* expression. Intriguingly, in the adult mouse brain, some hypothalamic neurons of the preoptic area, which senses body temperature (Boulant, 2000), express the TTX-1 related protein Otx2 (Kelley et al., 2000). Moreover, in the developing olfactory sensory epithelium Otx2 is expressed and largely restricted to the ensheathing glia (Mallamaci et al., 1996). Our finding that murine Otx2, but not Otx1, robustly restored *ver-1* expression to *ttx-1* mutants in *C. elegans* might, therefore, indicate that Otx2 has conserved roles in thermosensation and/or the function of glia in sensory organs, in addition to its other well-studied roles in development.

Acknowledgements

We thank P. Sengupta, B. Podbilewicz, W. Mohler, R. Barstead and the *C. elegans* Gene Knockout Consortium, and S. Mitani and the National Bioresource Project for strains. Other strains used in this study were provided by the *Caenorhabditis* Genetics Center, supported by the National Institutes of Health. We thank members of the Shaham lab for comments on the manuscript; E. Nudleman for construction of the thermotaxis apparatus; and D. Biron and A. Samuel for advice. A. Fire, M. Heiman, C. Popovici and R. Roubin provided plasmids. A. Singhvi and Y. Lu provided EM of the post-dauer adult. S.S. was a Klingenstein fellow in the neurosciences. This work was supported by grants R01HD052677 and R01NS064273 to S.S. Deposited in PMC for release after 12 months.

Competing interests statement

The authors declare no competing financial interests.

Supplementary material

Supplementary material for this article is available at <http://dev.biologists.org/lookup/suppl/doi:10.1242/dev.058305/-/DC1>

References

- Albert, P. S. and Riddle, D. L. (1983). Developmental alterations in sensory neuroanatomy of the *Caenorhabditis elegans* dauer larva. *J. Comp. Neurol.* **219**, 461-481.
- Bacaj, T., Tevlin, M., Lu, Y. and Shaham, S. (2008). Glia are essential for sensory organ function in *C. elegans*. *Science* **322**, 744-747.
- Bargmann, C. I. and Avery, L. (1995). Laser killing of cells in *Caenorhabditis elegans*. *Methods Cell Biol.* **48**, 225-250.
- Boulant, J. A. (2000). Role of the preoptic-anterior hypothalamus in thermoregulation and fever. *Clin. Infect. Dis.* **31 Suppl. 5**, S157-S161.
- Brenner, S. (1974). The genetics of *Caenorhabditis elegans*. *Genetics* **77**, 71-94.
- Canoll, P. and Goldman, J. E. (2008). The interface between glial progenitors and gliomas. *Acta Neuropathol.* **116**, 465-477.
- Carmona, M. A., Murai, K. K., Wang, L., Roberts, A. J. and Pasquale, E. B. (2009). Glial ephrin-A3 regulates hippocampal dendritic spine morphology and glutamate transport. *Proc. Natl. Acad. Sci. USA* **106**, 12524-12529.
- Coburn, C. M. and Bargmann, C. I. (1996). A putative cyclic nucleotide-gated channel is required for sensory development and function in *C. elegans*. *Neuron* **17**, 695-706.
- Colbert, H. A., Smith, T. L. and Bargmann, C. I. (1997). OSM-9, a novel protein with structural similarity to channels, is required for olfaction, mechanosensation, and olfactory adaptation in *Caenorhabditis elegans*. *J. Neurosci.* **17**, 8259-8269.
- Conradt, B. and Horvitz, H. R. (1998). The *C. elegans* protein EGL-1 is required for programmed cell death and interacts with the Bcl-2-like protein CED-9. *Cell* **93**, 519-529.
- Dunaevsky, A., Tashiro, A., Majewska, A., Mason, C. and Yuste, R. (1999). Developmental regulation of spine motility in the mammalian central nervous system. *Proc. Natl. Acad. Sci. USA* **96**, 13438-13443.
- Estevez, M., Attisano, L., Wrana, J. L., Albert, P. S., Massague, J. and Riddle, D. L. (1993). The *daf-4* gene encodes a bone morphogenetic protein receptor controlling *C. elegans* dauer larva development. *Nature* **365**, 644-649.

- Feldman, D. E.** (2009). Synaptic mechanisms for plasticity in neocortex. *Annu. Rev. Neurosci.* **32**, 33-55.
- Fraser, A. G., Kamath, R. S., Zipperlen, P., Martinez-Campos, M., Sohrmann, M. and Ahringer, J.** (2000). Functional genomic analysis of *C. elegans* chromosome I by systematic RNA interference. *Nature* **408**, 325-330.
- Georgi, L. L., Albert, P. S. and Riddle, D. L.** (1990). *daf-1*, a *C. elegans* gene controlling dauer larva development, encodes a novel receptor protein kinase. *Cell* **61**, 635-645.
- Golden, J. W. and Riddle, D. L.** (1984). The *Caenorhabditis elegans* dauer larva: developmental effects of pheromone, food, and temperature. *Dev. Biol.* **102**, 368-378.
- Hedgecock, E. M. and Russell, R. L.** (1975). Normal and mutant thermotaxis in the nematode *Caenorhabditis elegans*. *Proc. Natl. Acad. Sci. USA* **72**, 4061-4065.
- Holtmaat, A. and Svoboda, K.** (2009). Experience-dependent structural synaptic plasticity in the mammalian brain. *Nat. Rev. Neurosci.* **10**, 647-658.
- Huang, L. S., Tzou, P. and Sternberg, P. W.** (1994). The *lin-15* locus encodes two negative regulators of *Caenorhabditis elegans* vulval development. *Mol. Biol. Cell* **5**, 395-411.
- Inada, H., Ito, H., Satterlee, J., Sengupta, P., Matsumoto, K. and Mori, I.** (2006). Identification of guanylyl cyclases that function in thermosensory neurons of *Caenorhabditis elegans*. *Genetics* **172**, 2239-2252.
- Kelley, C. G., Lavorgna, G., Clark, M. E., Boncinelli, E. and Mellon, P. L.** (2000). The *Otx2* homeoprotein regulates expression from the gonadotropin-releasing hormone proximal promoter. *Mol. Endocrinol.* **14**, 1246-1256.
- Kimura, K. D., Tissenbaum, H. A., Liu, Y. and Ruvkun, G.** (1997). *daf-2*, an insulin receptor-like gene that regulates longevity and diapause in *Caenorhabditis elegans*. *Science* **277**, 942-946.
- Kimura, K. D., Miyawaki, A., Matsumoto, K. and Mori, I.** (2004). The *C. elegans* thermosensory neuron AFD responds to warming. *Curr. Biol.* **14**, 1291-1295.
- Komatsu, H., Mori, I., Rhee, J. S., Akaike, N. and Ohshima, Y.** (1996). Mutations in a cyclic nucleotide-gated channel lead to abnormal thermosensation and chemosensation in *C. elegans*. *Neuron* **17**, 707-718.
- Kumar, S. V. and Wigge, P. A.** (2010). H2A.Z-containing nucleosomes mediate the thermosensory response in *Arabidopsis*. *Cell* **140**, 136-147.
- Lippman, J. J., Lordkipanidze, T., Buell, M. E., Yoon, S. O. and Dunaevsky, A.** (2008). Morphogenesis and regulation of Bergmann glial processes during Purkinje cell dendritic spine ensheathment and synaptogenesis. *Glia* **56**, 1463-1477.
- Lundquist, E. A., Reddien, P. W., Hartwig, E., Horvitz, H. R. and Bargmann, C. I.** (2001). Three *C. elegans* Rac proteins and several alternative Rac regulators control axon guidance, cell migration and apoptotic cell phagocytosis. *Development* **128**, 4475-4488.
- Mallamaci, A., Di Blas, E., Briata, P., Boncinelli, E. and Corte, G.** (1996). *OTX2* homeoprotein in the developing central nervous system and migratory cells of the olfactory area. *Mech. Dev.* **58**, 165-178.
- Mello, C. and Fire, A.** (1995). DNA transformation. *Methods Cell Biol.* **48**, 451-482.
- Mello, C. C., Kramer, J. M., Stinchcomb, D. and Ambros, V.** (1991). Efficient gene transfer in *C. elegans*: extrachromosomal maintenance and integration of transforming sequences. *EMBO J.* **10**, 3959-3970.
- Mohler, W. A., Shemer, G., del Campo, J. J., Valansi, C., Opoku-Serebuoh, E., Scranton, V., Assaf, N., White, J. G. and Podbilewicz, B.** (2002). The type I membrane protein EFF-1 is essential for developmental cell fusion. *Dev. Cell* **2**, 355-362.
- Mori, I. and Ohshima, Y.** (1995). Neural regulation of thermotaxis in *Caenorhabditis elegans*. *Nature* **376**, 344-348.
- Mukhopadhyay, S., Lu, Y., Shaham, S. and Sengupta, P.** (2008). Sensory signaling-dependent remodeling of olfactory cilia architecture in *C. elegans*. *Dev. Cell* **14**, 762-774.
- Murai, K. K., Nguyen, L. N., Irie, F., Yamaguchi, Y. and Pasquale, E. B.** (2003). Control of hippocampal dendritic spine morphology through ephrin-A3/EphA4 signaling. *Nat. Neurosci.* **6**, 153-160.
- Murakami, S. and Johnson, T. E.** (2001). The *OLD-1* positive regulator of longevity and stress resistance is under *DAF-16* regulation in *Caenorhabditis elegans*. *Curr. Biol.* **11**, 1517-1523.
- Okkema, P. G., Harrison, S. W., Plunger, V., Aryana, A. and Fire, A.** (1993). Sequence requirements for myosin gene expression and regulation in *Caenorhabditis elegans*. *Genetics* **135**, 385-404.
- Ozawa, K., Suchanek, G., Breitschopf, H., Bruck, W., Budka, H., Jellinger, K. and Lassmann, H.** (1994). Patterns of oligodendroglia pathology in multiple sclerosis. *Brain* **117**, 1311-1322.
- Peckol, E. L., Troemel, E. R. and Bargmann, C. I.** (2001). Sensory experience and sensory activity regulate chemosensory receptor gene expression in *Caenorhabditis elegans*. *Proc. Natl. Acad. Sci. USA* **98**, 11032-11038.
- Perens, E. A. and Shaham, S.** (2005). *C. elegans daf-6* encodes a patched-related protein required for lumen formation. *Dev. Cell* **8**, 893-906.
- Perkins, L. A., Hedgecock, E. M., Thomson, J. N. and Culotti, J. G.** (1986). Mutant sensory cilia in the nematode *Caenorhabditis elegans*. *Dev. Biol.* **117**, 456-487.
- Popovici, C., Isnardon, D., Birnbaum, D. and Roubin, R.** (2002). *Caenorhabditis elegans* receptors related to mammalian vascular endothelial growth factor receptors are expressed in neural cells. *Neurosci. Lett.* **329**, 116-120.
- Porter, J. T. and McCarthy, K. D.** (1996). Hippocampal astrocytes in situ respond to glutamate released from synaptic terminals. *J. Neurosci.* **16**, 5073-5081.
- Ren, P., Lim, C. S., Johnsen, R., Albert, P. S., Pilgrim, D. and Riddle, D. L.** (1996). Control of *C. elegans* larval development by neuronal expression of a TGF-beta homolog. *Science* **274**, 1389-1391.
- Riddle, D. L., Swanson, M. M. and Albert, P. S.** (1981). Interacting genes in nematode dauer larva formation. *Nature* **290**, 668-671.
- Roayaie, K., Crump, J. G., Sagasti, A. and Bargmann, C. I.** (1998). The G alpha protein ODR-3 mediates olfactory and nociceptive function and controls cilium morphogenesis in *C. elegans* olfactory neurons. *Neuron* **20**, 55-67.
- Ryu, W. S. and Samuel, A. D.** (2002). Thermotaxis in *Caenorhabditis elegans* analyzed by measuring responses to defined thermal stimuli. *J. Neurosci.* **22**, 5727-5733.
- Sapir, A., Choi, J., Leikina, E., Avinoam, O., Valansi, C., Chernomordik, L. V., Newman, A. P. and Podbilewicz, B.** (2007). *AFF-1*, a FOS-1-regulated fusogen, mediates fusion of the anchor cell in *C. elegans*. *Dev. Cell* **12**, 683-698.
- Satterlee, J. S., Sasakura, H., Kuhara, A., Berkeley, M., Mori, I. and Sengupta, P.** (2001). Specification of thermosensory neuron fate in *C. elegans* requires *ttx-1*, a homolog of *otd/Otx*. *Neuron* **31**, 943-956.
- Schummers, J., Yu, H. and Sur, M.** (2008). Tuned responses of astrocytes and their influence on hemodynamic signals in the visual cortex. *Science* **320**, 1638-1643.
- Shaham, S.** (2005). Glia-neuron interactions in nervous system function and development. *Curr. Top. Dev. Biol.* **69**, 39-66.
- Shaham, S.** (2010). Chemosensory organs as models of neuronal synapses. *Nat. Rev. Neurosci.* **11**, 212-217.
- Shimizu, H., Watanabe, E., Hiyama, T. Y., Nagakura, A., Fujikawa, A., Okado, H., Yanagawa, Y., Obata, K. and Noda, M.** (2007). Glial Nax channels control lactate signaling to neurons for brain [Na⁺] sensing. *Neuron* **54**, 59-72.
- Sondell, M., Lundborg, G. and Kanje, M.** (1999). Vascular endothelial growth factor has neurotrophic activity and stimulates axonal outgrowth, enhancing cell survival and Schwann cell proliferation in the peripheral nervous system. *J. Neurosci.* **19**, 5731-5740.
- Spacek, J.** (1985). Three-dimensional analysis of dendritic spines. III. Glial sheath. *Anat. Embryol. (Berl.)* **171**, 245-252.
- Theodosios, D. T. and Poulain, D. A.** (1993). Activity-dependent neuronal-glia and synaptic plasticity in the adult mammalian hypothalamus. *Neuroscience* **57**, 501-535.
- Timmons, L. and Fire, A.** (1998). Specific interference by ingested dsRNA. *Nature* **395**, 854.
- Ventura, R. and Harris, K. M.** (1999). Three-dimensional relationships between hippocampal synapses and astrocytes. *J. Neurosci.* **19**, 6897-6906.
- Wang, W. Y., Dong, J. H., Liu, X., Wang, Y., Ying, G. X., Ni, Z. M. and Zhou, C. F.** (2005). Vascular endothelial growth factor and its receptor Flk-1 are expressed in the hippocampus following entorhinal deafferentation. *Neuroscience* **134**, 1167-1178.
- Wang, Y., Apicella, A., Jr, Lee, S. K., Ezcurra, M., Slone, R. D., Goldmit, M., Schafer, W. R., Shaham, S., Driscoll, M. and Bianchi, L.** (2008). A glial DEG/ENaC channel functions with neuronal channel DEG-1 to mediate specific sensory functions in *C. elegans*. *EMBO J.* **27**, 2388-2399.
- Woolley, C. S., Gould, E., Frankfurt, M. and McEwen, B. S.** (1990). Naturally occurring fluctuation in dendritic spine density on adult hippocampal pyramidal neurons. *J. Neurosci.* **10**, 4035-4039.